

The Difficulty of Measuring Low Friction: Uncertainty Analysis for Friction Coefficient Measurements

Tony L. Schmitz, Jason E. Action, John C. Ziegert, and W. Gregory Sawyer

University of Florida, Department of Mechanical and Aerospace Engineering, Gainesville, FL 32611

The experimental evaluation of friction coefficient is a common laboratory procedure; however, the corresponding measurement uncertainty is not widely discussed. This manuscript examines the experimental uncertainty associated with friction measurements by following the guidelines prescribed in international standards. The uncertainty contributors identified in this analysis include load cell calibration, load cell voltage measurement, and instrument geometry. A series of 20 tests, carried out under nominally identical conditions, was performed using a reciprocating pin-on-disk tribometer. A comparison between the experimental standard deviation and uncertainty analysis results is provided.

[DOI: 10.1115/1.1843853]

1 Introduction

Laboratory experimentation remains the only practical method available for the accurate identification of friction coefficients for arbitrary material pairs. However, accurate and repeatable friction coefficient measurement remains challenging due to the dependence of friction coefficients on the material, surface, environment, and measuring equipment. The purpose of this paper is to critically examine the experimental uncertainty associated with the instrumentation used in dynamic friction coefficient measurements. In order to enable the confident use of experimental data, it is necessary to provide a quantitative, defensible statement regarding its reliability. The topic of data uncertainty has been addressed by researchers for several individual tribological measurement conditions [1–6]. In this paper, we focus on establishing a systematic framework for the evaluation of instrument-related uncertainty in tribological testing. Our example application is the determination of low dynamic coefficients of friction.

We consider friction coefficient measurements carried out using a traditional pin-on-disk tribometer, where a pin is pressed against a reciprocating counterface. This tribometer uses a pneumatic cylinder and a multichannel load cell located directly above the pin to continuously monitor the contact force vector, which is then decomposed into friction force and normal force vectors. The uncertainty analysis follows the guidelines provided in Refs. [7,8]. Uncertainty contributors include load cell calibration, where both the applied load and voltage measurement uncertainties have been considered, and instrument geometry.

2 Description of Tribology Experiments

2.1 Reciprocating Pin-on-Disk Tribometer. The tribometer shown schematically in Fig. 1 creates a reciprocating sliding contact between two surfaces of interest. A four-shaft pneumatic thruster, model 64a-4 produced by Ultramation (Specific commercial equipment is identified to fully describe the experimental procedures. This identification does not imply endorsement by the authors.), creates the loading conditions of the contact using a 61.2 mm bore Bimba pneumatic cylinder. The cylinder is nomi-

nally protected from transverse loads by four 12 mm diameter steel rods. An electro-pneumatic pressure regulator controls the force produced by the thruster. The pneumatic pressure output is controlled by a variable voltage input and the desired pressure output is maintained by an active control loop within the electro-pneumatic system. A linear positioning table is used to create the reciprocating motion between the stationary pin and counterface. The positioning system is composed of a table, ball screw, and stepper motor; sliding speeds up to 152 mm/s are possible. The force created by the thruster and friction force generated by the contact is monitored using a six-axis force transducer. This load cell, which is mounted under the thruster, monitors forces created in the X , Y , and Z -axes as well as the moments about these axes. The transducer output voltages are recorded using a computer data acquisition system (500 Hz sampling rate).

2.2 Experimental Procedure. Twenty experiments were conducted using a polytetrafluoroethylene (PTFE) pin and polished 347 stainless steel counterface. Every effort was made to maintain identical test conditions. Commercial PTFE rod stock was machined to produce 6.35 mm \times 6.35 mm \times 12.7 mm pin samples, which were mounted in the sample holder and machined flat. The initial mass of the sample-holder was recorded. The 347 stainless steel counterface was wet-sanded with 600 grit sandpaper, cleaned with soap and water, and wiped with alcohol prior to each test. All counterface surfaces were examined using a scanning white-light interferometer to verify an average roughness (R_a) between 0.1 and 0.2 μm .

During testing, a 175 N normal force was maintained using the load cell's force level as feedback to the pneumatic cylinder air supply via an inline electro-pneumatic valve. The average contact pressure for these tests was approximately 4.35 MPa. Tests were carried out for approximately 90 minutes, during which 2400 cycles were commanded over a 50.8 mm path length.

3 Friction Coefficient Calculations

The instantaneous coefficient of friction (μ) is defined as the ratio of the measured friction force, (F_f) to the measured normal force (F_n) as shown in Eq. (1),

$$\mu = \frac{F_f}{F_n} \quad (1)$$

Typically, the friction and normal forces at the contact are measured separately using some combination of force transducers and/or dead weight loads. Misalignments between the force measurement axes and the directions normal (N) and tangent (T) to the reciprocating or rotating surface constitute one of the most significant contributors to friction coefficient measurement errors. Figure 2 shows the misalignment geometry.

Here, the normal and tangential directions are defined by the surface of the counterface. The intent of the instrument designer is to measure forces along these directions. However, manufacturing tolerances inevitably produce some misalignment between the axes of the force measurement system and the normal and tangential axes. In Fig. 2, the transducer axis that is intended to measure the normal force is designated by Y and is misaligned by an angle β ; the transducer axis that is intended to measure the tangential force is designated by X and is misaligned by an angle α . In this general case, the measurement axes are not assumed to be perpendicular. The normal and tangential components of the contact force may be projected onto the measurement axes, resulting in the measured forces (F_X, F_Y) defined in Eq. (2).

$$F_X = F_f \cos \alpha + F_n \sin \alpha = F_n (\sin \alpha + \mu \cos \alpha)$$

$$F_Y = F_n \cos \beta - F_f \sin \beta = F_n (\cos \beta - \mu \sin \beta) \quad (2)$$

Contributed by the Tribology Division for publication in the ASME JOURNAL OF TRIBOLOGY. Manuscript received by the Tribology Division August 24, 2004; revised manuscript received August 27, 2004. Review conducted by: J. Tichy.

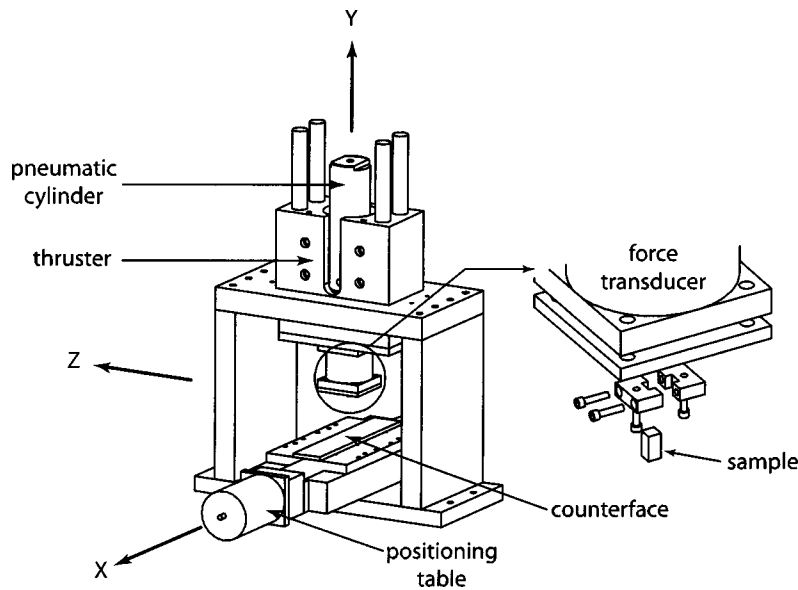


Fig. 1 Schematic of the reciprocating tribometer constructed for this study

Using these projections, a solution for the friction coefficient in terms of the measured forces and misalignment angles (α , β) can be derived; this is shown in Eq. (3).

$$\mu = \frac{F_X \cos \beta - F_Y \sin \alpha}{F_Y \cos \alpha + F_X \sin \beta} \quad (3)$$

The misalignment angles are typically assumed to be zero and the coefficient of friction is computed directly as the ratio of the measured X direction force to the measured Y direction force, i.e., $\mu' = F_X/F_Y$. The error fraction (E) associated with making such an assumption is defined in Eq. (4), where μ is given by Eq. (3).

$$E = \frac{\mu - \mu'}{\mu} = \frac{\mu \cos \beta - \mu^2 \sin \beta - \mu \cos \alpha - \sin \alpha}{\mu \cos \beta - \mu^2 \sin \beta} \quad (4)$$

For the reciprocating tribometer described in Sec. 2.1, the X and Y direction forces are measured by a multi-axis force transducer. As-

suming the transducer axes are perpendicular (i.e., $\alpha = \beta$), Eq. (4) reduces to Eq. (5). An associated error plot is shown in Fig. 3.

$$E = \frac{\mu^2 \sin \alpha + \sin \alpha}{\mu^2 \sin \alpha - \mu \cos \alpha} \quad (5)$$

For a well-designed instrument, the misalignment angle (α) is small, and small angle approximations for the sine and cosine terms can be applied in Eq. (5), giving Eq. (6).

$$E = \frac{2\alpha(1 + \mu^2)}{\mu(\alpha^2 + 2\mu\alpha - 2)} \quad (6)$$

For any given misalignment angle the error increases with a decreasing friction coefficient. Equation (6) can be further simplified by dropping higher order terms to give Eq. (7).

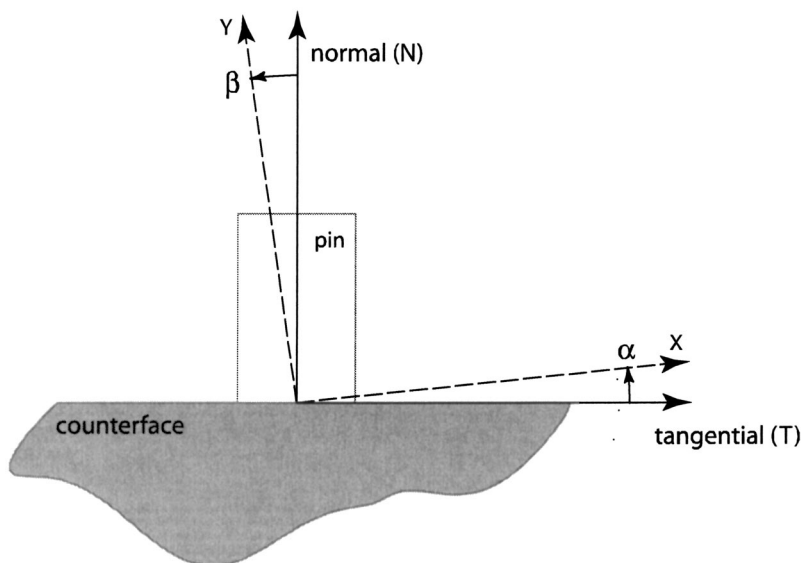


Fig. 2 A sketch of the force measurement geometry, where the misalignment angles α and β are not necessarily equal

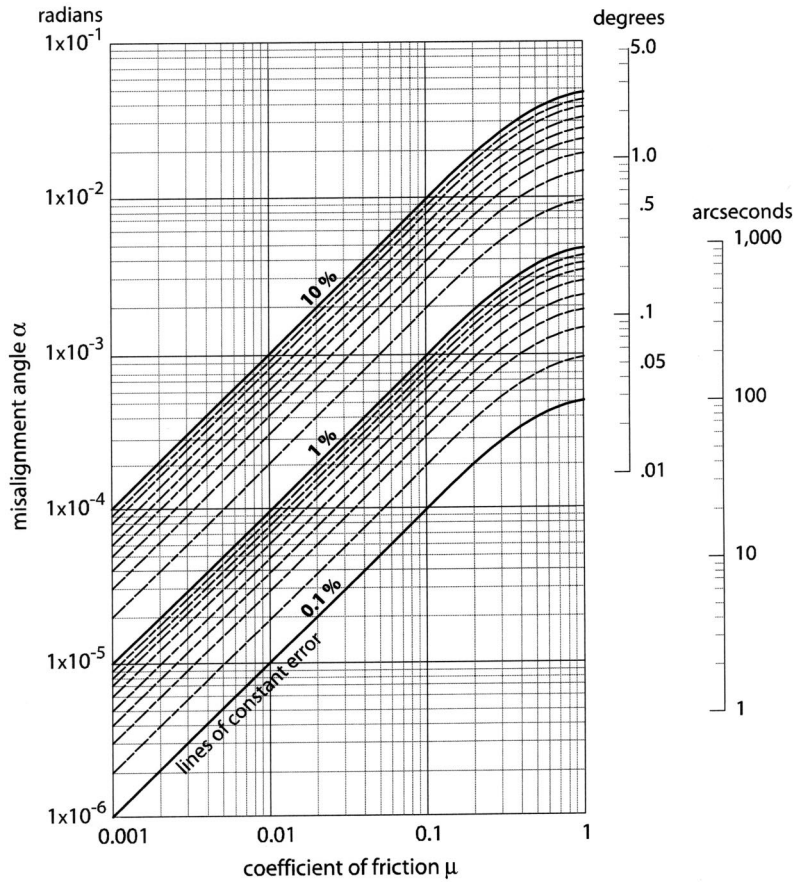


Fig. 3 An error graph, showing lines of constant error as a function of misalignment angle α , where β is assumed to be equal to α

$$E = \frac{-\alpha}{\mu} \quad (7)$$

The implications of Eq. (7) are clear. When the friction coefficient is small, the transducer axes must be nearly perfectly aligned to the normal and tangential axes in order to prevent large errors.

4 Uncertainty of Dynamic Friction Coefficient Measurements

When reporting friction coefficients, as with any measured quantity, it is also necessary to provide a quantitative statement regarding the quality of the reported value so that those who wish to use the data can have an indication of its reliability. The “*dispersion of values that could reasonably be attributed to the measurand*” [7] is the measurement uncertainty. An uncertainty analysis is the procedure used to determine the uncertainty of a measurement and recommendations for carrying out such analyses are described Refs. [7,8], which were used here.

For our measurements, the measurand, μ , is not observed directly, but is determined from Eq. (3), which includes the measured forces F_X and F_Y and estimates of the misalignment angles, α and β . Prior to carrying out any uncertainty analysis, the known errors (biases) must be corrected or compensated. In this case, the misalignment errors must be treated so that the reported value of μ is not subject to the systematic errors described in Sec. 3. However, even after all known error sources in the measurement have been evaluated and corrected or compensated, residual uncertainty in the reported result remains due to the uncertainties in the measurements of the individual input quantities; in Eq. (3), the quantities are F_X , F_Y , α , and β .

In order to evaluate the measurement uncertainty for μ , we apply the *law of propagation of uncertainty* to determine the combined standard uncertainty, u_c , which represents one standard deviation of the friction coefficient measurement result. The combined standard uncertainty is a function of the standard uncertainty of each input measurement and the associated sensitivity coefficients, or partial derivatives of the functional relationship between the friction coefficient and input quantities, with respect to each input quantity. These partials are evaluated at nominal values of the input quantities.

The expression for the square of the combined standard uncertainty in our friction coefficient result is provided in Eq. (8), where the standard uncertainty in each input variable ($u(x)$) can be determined using Type-A or Type-B uncertainty evaluations. In Type-A, statistical methods are employed and the standard uncertainty is determined by the experimental standard deviation of the measured values. Type-B evaluations involve all other methods, including data supplied with a particular transducer and engineering judgment. Equation (8) does not contain the potential for correlation (or dependence) between the separate input variables; zero covariance has been assumed in this analysis, as is often the case.

$$u_c^2(\mu) = \left(\frac{\partial \mu}{\partial F_X}\right)^2 u^2(F_X) + \left(\frac{\partial \mu}{\partial F_Y}\right)^2 u^2(F_Y) + \left(\frac{\partial \mu}{\partial \alpha}\right)^2 u^2(\alpha) + \left(\frac{\partial \mu}{\partial \beta}\right)^2 u^2(\beta) \quad (8)$$

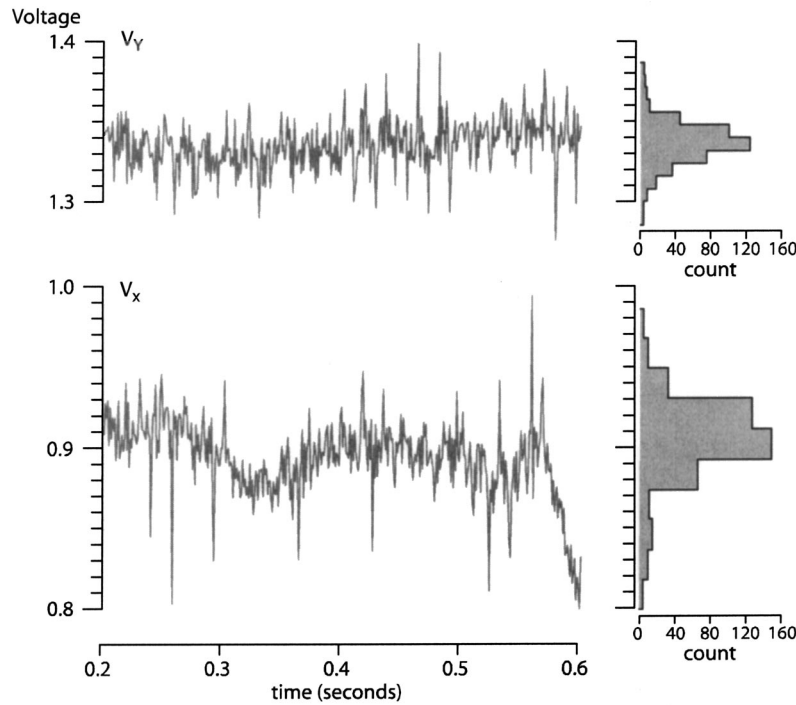


Fig. 4 Sample raw data (in Volts) from the load cell/conditioner pair during an experiment

The partial derivatives of the friction coefficient [as shown in Eq. (4)] with respect to the input variables F_X , F_Y , α , and β are given by Eqs. (9)–(12), respectively.

$$\frac{\partial \mu}{\partial F_X} = \frac{\cos(\beta)}{F_Y \cos(\alpha) + F_X \sin(\beta)} - \frac{\sin(\beta)[F_X \cos(\beta) - F_Y \sin(\alpha)]}{[F_Y \cos(\alpha) + F_X \sin(\beta)]^2} \quad (9)$$

$$\frac{\partial \mu}{\partial F_Y} = \frac{-\sin(\alpha)}{F_Y \cos(\alpha) + F_X \sin(\beta)} - \frac{\cos(\alpha)[F_X \cos(\beta) - F_Y \sin(\alpha)]}{[F_Y \cos(\alpha) + F_X \sin(\beta)]^2} \quad (10)$$

$$\begin{aligned} \frac{\partial \mu}{\partial \alpha} &= \frac{-F_Y \cos(\alpha)}{F_Y \cos(\alpha) + F_X \sin(\beta)} \\ &+ \frac{F_Y \sin(\alpha)[F_X \cos(\beta) - F_Y \sin(\alpha)]}{[F_Y \cos(\alpha) + F_X \sin(\beta)]^2} \end{aligned} \quad (11)$$

$$\begin{aligned} \frac{\partial \mu}{\partial \beta} &= \frac{-F_X \sin(\beta)}{F_Y \cos(\alpha) + F_X \sin(\beta)} \\ &- \frac{F_X \cos(\beta)[F_X \cos(\beta) - F_Y \sin(\alpha)]}{[F_Y \cos(\alpha) + F_X \sin(\beta)]^2} \end{aligned} \quad (12)$$

In the following sections, we detail our evaluations of the standard uncertainties for the input quantities. These values are then substituted into Eq. (8), with the partials [Eqs. (9)–(12)] evaluated at the nominal operating conditions for the testing carried out here. Finally, the numerical value for the combined standard uncertainty is calculated for this tribometer, although the methodology is generic and can be applied to other tribometers as well.

4.1 Standard Uncertainty of Force Calibration. For the reciprocating tribometer, a multi-axis force transducer manufactured by Advanced Mechanical Technology, Inc. is used to measure the contact force. The MC3A-6-500 transducer is capable of measuring forces in three nominally orthogonal axes as well as moments about these axes. This force transducer has a maximum load capacity of 2200 N along the Y -axis (vertical direction) and

an 1100 N capacity in the X and Z axes. The transducer and conditioner pair output a voltage, V_i , which is then multiplied by a calibration constant, C_i , to obtain the desired force values.

$$F_X = C_X V_X$$

$$F_Y = C_Y V_Y \quad (13)$$

In general, crosstalk exists between the force transducer axes, requiring a matrix relationship between the reported forces and moments, measured voltages, and calibration constants. This is given by Eq. (14), where $\{V_j\}$ is the 6 component vector of transducer output voltages, $\{F_k\}$ is the 6 component vector of forces and moments, and $[C_{jk}]$ is the 6×6 crosstalk matrix. For the transducer used in these experiments, the crosstalk between any pair of axes was 2% or less according to the manufacturer and was, therefore, neglected.

$$\{F_j\} = [C_{jk}] \{V_k\} \quad (14)$$

The X and Y direction calibration constants for the force transducer were determined by applying known dead weight loads to the channel of interest on the transducer and recording the corresponding voltage. The slope of the applied force versus voltage trace was then taken to be the calibration constant for that axis.

The uncertainty in the measured calibration constants is dependent on the uncertainties in both the measured voltages and the forces applied during the calibration sequence. The voltages were recorded using a 12-bit data acquisition card with an operating range of 20 V. The resulting quantization error (\pm least significant bit), ΔV , is 4.9 mV. The dead weight loads were measured on a digital scale with an uncertainty of 0.025 N. Because there are uncertainties in both voltage and load, a Monte Carlo simulation was completed to generate calibration curves based on both the mean and standard uncertainty for the dead weight values and recorded voltages (normal distributions were assumed for each uncertainty). The mean and standard deviation of the calibration constants for the transducer X direction were 35.99 N/V and

Table 1 Values used in the friction coefficient combined standard uncertainty calculation

Input	Nominal Value	Standard Uncertainty, u_i	Sensitivity, s_i	$u_i s_i$
\bar{F}_X	30 N	0.095 (N)	5.65×10^{-3} (1/N) [Eq. (9)]	5.37×10^{-4}
\bar{F}_Y	175 N	0.541 (N)	-0.98×10^{-3} (1/N) [Eq. (10)]	-5.30×10^{-4}
α^a	0.0428	0.349×10^{-3}	-0.987 [Eq. (11)]	-3.44×10^{-4}
β^a	0.0428	0.349×10^{-3}	-0.030 [Eq. (12)]	-0.10×10^{-4}
Combined standard uncertainty, $u_c(\mu)$ [Eq. (8)]				8.3×10^{-4}

^aAll angles reported in radians.

0.11 N/V and 148.77 N/V and 0.39 N/V for the Y direction. These standard deviations were taken to be the best estimate of the calibration constant uncertainties.

4.2 Standard Uncertainty of Voltage Measurements.

During experiments the X and Y direction transducer voltages were subject to Gaussian, or normally distributed, noise. The presence of this noise makes it inappropriate to compute the friction coefficient based on a single point force measurement. Thus, the friction coefficient was computed using time-averaged transducer voltages. The uncertainty in the average measured voltages was obtained using Eqs. (15) and (16), where $s^2(V_X)$ and $s^2(V_Y)$ are the variances in the voltages recorded by the force transducer in the X and Y directions, respectively, n is the number of samples, and \bar{V}_X and \bar{V}_Y are the mean recorded voltages in the X and Y directions, respectively [9].

$$u^2(\bar{V}_X) = \frac{s^2(V_X)}{n} = \frac{1}{n-1} \frac{\sum_{i=1}^n (V_{X,i} - \bar{V}_X)^2}{n} \quad (15)$$

$$u^2(\bar{V}_Y) = \frac{s^2(V_Y)}{n} = \frac{1}{n-1} \frac{\sum_{i=1}^n (V_{Y,i} - \bar{V}_Y)^2}{n}. \quad (16)$$

For the typical data shown in Fig. 4, the mean voltage values were 0.893 V for the X direction and 1.336 V for the Y direction. This data was collected near the midpoint of the reciprocating path stroke. The standard uncertainties in these average values were 1.53×10^{-6} V and 6.07×10^{-7} V for the X and Y directions, respectively.

4.3 Standard Uncertainty of Forces. As previously discussed, average X and Y -direction force values, \bar{F}_X and \bar{F}_Y , were used in the friction coefficient calculations due to the normally distributed noise in the experimental data. These forces were calculated using Eq. (17)

$$\bar{F}_X = \frac{C_X}{n} \sum_{i=1}^n V_{X,i} = C_X \bar{V}_X \quad \bar{F}_Y = \frac{C_Y}{n} \sum_{i=1}^n V_{Y,i} = C_Y \bar{V}_Y \quad (17)$$

The standard uncertainties in the mean values \bar{F}_X and \bar{F}_Y are given by Eqs. (18) and (19), respectively.

$$u^2(\bar{F}_X) = \left(\frac{\partial \bar{F}_X}{\partial C_X} \right)^2 u^2(C_X) + \left(\frac{\partial \bar{F}_X}{\partial \bar{V}_X} \right)^2 u^2(\bar{V}_X) \\ = (\bar{V}_X)^2 u^2(C_X) + (C_X)^2 u^2(\bar{V}_X) \quad (18)$$

$$u^2(\bar{F}_Y) = \left(\frac{\partial \bar{F}_Y}{\partial C_Y} \right)^2 u^2(C_Y) + \left(\frac{\partial \bar{F}_Y}{\partial \bar{V}_Y} \right)^2 u^2(\bar{V}_Y) \\ = (\bar{V}_Y)^2 u^2(C_Y) + (C_Y)^2 u^2(\bar{V}_Y) \quad (19)$$

The calibration constant uncertainties (Sec. 4.1) and the average voltages measured during the friction coefficient testing (Sec. 4.2) were substituted in Eqs. (18) and (19) to obtain the uncertainties

in the average force values. For the test configuration and procedure described here $u(\bar{F}_X) = 0.095$ N and $u(\bar{F}_Y) = 0.541$ N.

4.4 Transducer Axis Misalignment Uncertainty. The angular misalignment for our test setup was determined by measuring the horizontal force produced by the application of a known vertical force. The mean angle of misalignment was found to be 2.45 deg from multiple repetitions using three different normal loads of 47.2 N, 92.6 N, and 138.2 N. The mean and standard deviation values, 2.45 deg and 0.02 deg, respectively, obtained from this sample distribution were assumed to provide the best estimates for the parent population mean and standard deviation so that $u(\alpha) = 0.02$ deg. Further, it was assumed that the transducer axes were perpendicular, such that $u(\alpha) = u(\beta) = 0.02$ deg.

5 Combined Standard Uncertainty

The combined standard uncertainty of the friction coefficient was obtained using Eq. (8), where F_X and F_Y are replaced by \bar{F}_X and \bar{F}_Y , respectively. The partial derivatives shown in Eqs. (9)–(12) were evaluated at the nominal operating conditions (i.e., the mean values described in previous sections) to obtain the sensitivity coefficients, s_i . Table 1 provides a summary of the nominal input parameters and associated uncertainties for the combined standard uncertainty $u_c(\mu)$, which is calculated as the square root of the sum of squares of the $u_i s_i$ terms. Again, we have assumed zero covariance between input values, so this summing method is valid.

The combined standard uncertainty for the friction coefficient measurement, $u_c(\mu)$, is 8.3×10^{-4} . The nominal value computed from Eq. (3) is $\mu = 0.127$. Thus, the standard uncertainty is approximately 0.7% of the nominal value. The expanded uncertainty for a greater than 99% confidence level (i.e., three standard deviations) is 24.93×10^{-4} , or $\sim 2\%$ of the nominal value. The reader may note that if the friction coefficient were calculated using only the ratio of the average forces ($\mu' = \bar{F}_X / \bar{F}_Y$) the resulting value would be 0.171; in this case, an uncorrected angular misalignment bias would produce a greater than 34% error. To demonstrate the validity of the uncertainty analysis, a Monte Carlo simulation was completed. For 10,000 calculations, the mean value of friction coefficient was 0.127 with a standard deviation of 7.6×10^{-4} , which agrees with the analytic derivation.

6 Discussion

A simple model that reveals the challenges associated with making measurements of low friction materials was described in Sec. 3. The model shows that the measurement of friction is extremely sensitive to angular misalignments between the loading axes and the counterface surfaces. For materials with friction coefficients below 0.05 the alignment becomes almost hopelessly difficult if the goal is to have uncertainties below 1%.

For the tests completed in this study, the friction coefficients were below 0.2. While the scatter in the data is clearly apparent (see Fig. 5), not all of this scatter can be attributed to uncertainties attributed to the experimental apparatus. In fact, the greatest source of variations in these measurements comes from the sub-

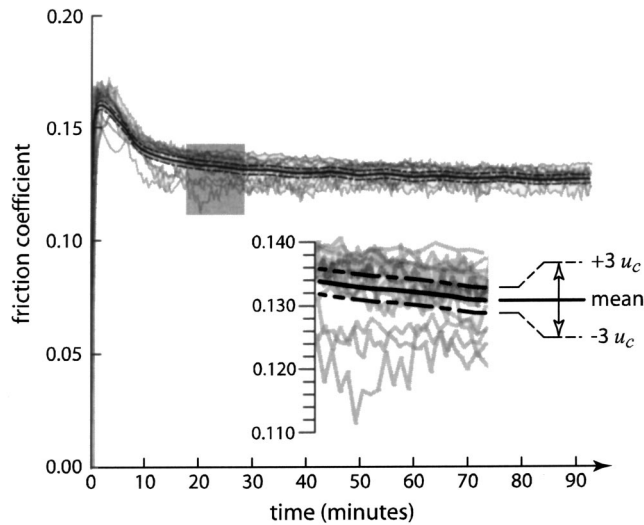


Fig. 5 Graph of the collected friction coefficient traces. The mean value from this data is shown by the dark solid line; the >99% confidence interval is shown by the dashed lines.

stantial number of factors that influence friction and the difficulty in controlling all of these variables. However, without knowledge of the instrument capabilities, it is impossible to distinguish between, for example, material variations and limitations of the tribometer.

The uncertainty analysis reported here can be used to understand the relative importance of the various contributors to instrument-related uncertainty in dynamic friction measurements. It may also help instrument designers focus on the most important factors in order to improve instrument accuracy and may also serve as a template for tribologists to follow in evaluating the uncertainty in their tribometers.

7 Conclusions

For material pairs that exhibit low friction, it was shown that very small misalignment of the force transducer axes relative to

the surface under test could produce large relative errors in the estimated friction coefficient unless those misalignments are quantified and the resulting error is compensated.

This paper outlined a general methodology for evaluating the instrument-related uncertainty of coefficient of friction measurements carried out on a reciprocating tribometer. Contributors to measurement uncertainty included calibration of the force transducers, misalignment of the transducer axes to the tribometer axes, and voltage measurement uncertainties in the data recording system.

Acknowledgments

This material is based upon work supported by the National Science Foundation under Grant No. CMS-0219889, "GOALI: Collaborative Research: Tribology of Nanocomposites." Any opinions, findings, and conclusions or recommendations expressed in this material are those of the authors and do not necessarily reflect the views of the National Science Foundation. The authors would like to acknowledge helpful discussions with Dr. Angela Davies, UNCC, during the completion of this work.

References

- [1] Parkins, D. W., 1995, "Measurement of Oil Film Journal Bearing Damping Coefficients-An Extension of the Selected Orbit Technique," *J. Tribol.*, **117**, pp. 696–701.
- [2] Sehgal, R., Gandhi, O. P., and Angra, S., 2001, "Wear Evaluation and Ranking of Tribomaterials Using a Hasse Diagram Approach," *J. Tribol.*, **123**, pp. 486–493.
- [3] Al-Qutub, A. M., Elrod, D., and Coleman, H. W., 2000, "A New Friction Factor Model and Entrance Loss Coefficient for Honeycomb Annular Gas Seals," *J. Tribol.*, **122**, pp. 622–627.
- [4] Ransom, D., Li, J. M., Andres, L. S., and Vance, J., 1999, "Experimental Force Coefficients for a Two-Bladed Labyrinth Seal and a Four-Pocket Damper Seal," *J. Tribol.*, **121**, pp. 370–376.
- [5] Tieu, A. K., and Qiu, Z. L., 1996, "Experimental Study of Freely Alignable Journal Bearings.1. Static Characteristics," *J. Tribol.*, **118**, pp. 498–502.
- [6] Qiu, Z. L., and Tieu, A. K., 1996, "Experimental Study of Freely Alignable Journal Bearings.2. Dynamic Characteristics," *J. Tribol.*, **118**, pp. 503–508.
- [7] "Guide to the Expression of Uncertainty in Measurement," 1993, International Standards Organization (ISO).
- [8] Taylor, B. N. and Kuyatt, C. E., Guidelines for Evaluating and Expressing the Uncertainty of Nist Measurement Results. in NIST Technical Note 1297, 1994.
- [9] Bevington, P. R. and Robinson, D. K., 1992, *Data Reduction and Error Analysis for the Physical Sciences*, 2nd ed., McGraw-Hill, Boston, MA.